Design and Optical Properties of Active Polymer-Coated Plasmonic Nanostructures

ARTICLE *in* JOURNAL OF PHYSICAL CHEMISTRY LETTERS · APRIL 2011

Impact Factor: 7.46 · DOI: 10.1021/jz200272r

8 AUTHORS, INCLUDING:

Georges Lévi
Paris Diderot University
75 PUBLICATIONS **2,106** CITATIONS
SEE PROFILE

Emmanuelle Lacaze
Pierre and Marie Curie University - Paris 6
92 PUBLICATIONS **1,270** CITATIONS
SEE PROFILE

THE JOURNAL OF PHYSICAL CHEMISTRY Letters

LETTER

pubs.acs.org/JPCL

Design and Optical Properties of Active Polymer-Coated Plasmonic Nanostructures

Hélène Gehan,[†] Claire Mangeney,[†] Jean Aubard,[†] Georges Lévi,[†] Andreas Hohenau,[‡] Joachim R. Krenn,[‡] Emmanuelle Lacaze,[§] and Nordin Félidj*[,†]

[†]Laboratoire ITODYS, Université Paris Diderot, CNRS UMR 7086, 15 rue Jean de Baïf, 75013 Paris, France

[‡]Institute of Physics, Karl Franzens University, Universitatsplatz 5, A-8010 Graz, Austria

[§]Laboratoire INSP, Université Pierre et Marie Curie, 5 place Jussieu, 75005 Paris, France

ABSTRACT: The grafting of stimuli-responsive polymer brushes on plasmonic structures provides a perfectly controlled two-dimensional active device with optical properties that can be modified through external stimuli. Herein, we demonstrate thermally induced modifications of the plasmonic response of lithographic gold nanoparticles functionalized by thermosensitive polymer brushes of (poly(*N*-isopropylacrylamide), PNIPAM). Optical modifications result from refractive local index changes due to a phase transition from a hydrophilic state (swollen regime) to a hydrophobic state (collapsed regime) of the polymer chains occurring in a very small range of temperatures. The refractive index of the polymer in aqueous solution is estimated in both states, deduced from the discrete dipole approximation (DDA) method. The combination of lithographic gold NPs and thermoresponsive polymer chains leads to a new generation of perfectly calibrated and dynamically controlled hybrid gold/polymer system for real-time nanosensors.

SECTION: Nanoparticles and Nanostructures

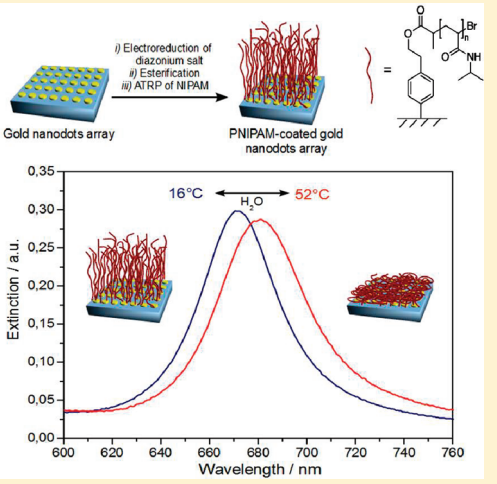

Noble-metal nanoparticles (NPs), mainly gold, silver, and copper, have generated intense and growing interest in the past decade owing to their rich optical properties.[1] A wide range of applications in nano-optics and ultrasensitive spectroscopies include guiding light on the submicrometer scale, light sources, filters, surface-enhanced Raman scattering or fluorescence, and biosensing.[2−5] These properties are related to localized surface plasmon resonance (LSPR), resulting in a high degree of optical field confinement with high sensitivity to their local environment.

The LSPR wavelength can be changed with the NPs' size and shape and their spacing, which is of main importance in the context of nano-optical applications.[2−7] To modify the LSPR wavelength without affecting the NPs' morphology, an interesting approach consists of modifying the surrounding medium characterized by its refractive index (RI). Therefore, many groups have considered the importance of achieving stimulable plasmonic systems using active materials as a surrounding medium, providing a continuous and reversible modulation of the plasmonic response.[8−11] For instance, LSPR wavelength reversible shifts were achieved by electrochemically changing the RI of conducting polymer films surrounding the NPs.[10] Liquid crystal templates were also shown to be excellent materials for active plasmonic devices due to their controllable birefringence.[12,13]

Stimuli-responsive polymer brushes are very efficient candidates in active plasmonics because the conformation of polymeric chains can be controlled by pH, ionic strength, and temperature.[14−18] If the polymer is bound to noble-metal nanostructures, the stimuli-induced conformational changes of the polymer can modify drastically the RI of the NPs' surrounding medium and, consequently, their optical properties.[19−22] For instance, I. Tokareva et al. studied the pH-induced swelling of polymer brushes by taking advantage of the extreme sensitivity of gold island films coupled to gold colloidal NPs.[19] Therefore, metallic NPs can be employed as molecular recognition elements in molecular sensing due to the strong sensitivity of the LSPR with respect to the local environment.

Significant progress has been made in mixing gold nanoparticles with polymer brushes.[23−28] However, until now, most of the reported experiments dealt with gold colloidal NPs or island films attached to polymer brushes. The optical response of these substrates leads to broad LSPR bands, thus preventing any improvement in analytical applications such as chemical sensoring or surface-enhanced spectroscopies.[5] In order to improve plasmonic system performances, one should consider two main issues, (i) fabrication of perfectly calibrated systems with controlled particle shape and size for a fine-tuning of the LSPR bands and (ii) control of the polymer grafting steps for optimization of the stimuli-induced response of the polymer with high grafted density of polymer brushes, strongly attached to the surface. We

Received: March 1, 2011
Accepted: April 4, 2011

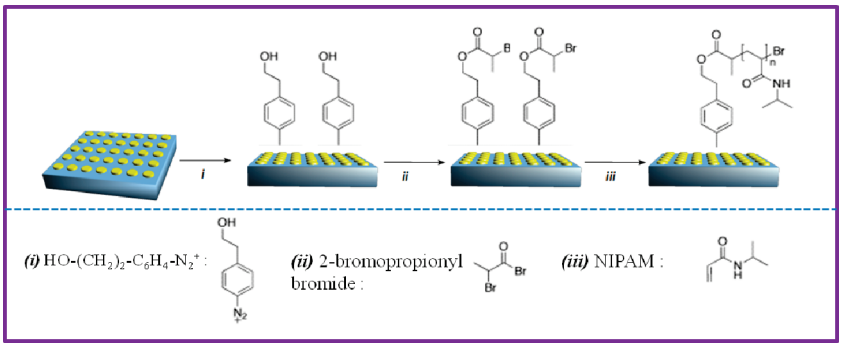

Figure 1. Fabrication of PNIPAM-grafted brushes on lithographic gold nanodot arrays. (i) Electroreduction of $HO-(CH_2)_2-C_6H_4-N_2^+$ salts on the substrate, (ii) esterification by 2-bromopropionyl bromide, and (iii) ATRP of NIPAM on the initiator-modified gold substrates.

thus expect a fine control of the LSPR wavelength through the modification of the external stimulus, making our system a very good candidate for real-time nanosensors.

In this Letter, we address the issue by analyzing the optical properties of a hybrid plasmonic device based on stimuli-responsive brushes grafted to lithographically designed gold nanostructures. Among stimulus-responsive polymers, the poly(*N*-isopropylacrilamide) (PNIPAM) is a thermosensitive polymer that undergoes a reversible phase transition upon going from a hydrophilic swollen conformational state to a hydrophobic collapsed state around its lower critical solution temperature (LCST) at 32 °C in pure water.[29] Conformational changes of PNIPAM brushes when varying the temperature are expected to induce significant modifications of the NPs' optical properties. We combined regular arrays of gold NPs with such PNIPAM brushes and studied the optical response of such systems as a function of the temperature. The RI of the PNIPAM was estimated, below and above the LCST, using the discrete dipole approximation (DDA) method, emphasing the idea that such structures may act as efficient real-time nanosensors.

Gold nanodots arrays were fabricated using electron beam lithography (EBL) on an indium−tin oxide (ITO)-covered glass substrate, enabling the control of the particle shape and size as well as their arrangement on the substrate. The details of this procedure are described elsewhere.[30] In the present work, the samples are made of a hexagonal array of gold circular dots (150 nm diameter and 45 nm height), with a grating constant (NPs' center to center) of 350 nm.

Our stepwise strategy for surface modification of gold NP arrays is shown in Figure 1, and the detailed procedure was previously described elsewhere.[31] Briefly, it involves the following steps: (i) The substrates are treated by an electrochemical reduction of 4-hydroxyethylbenzene diazonium tetrafluoroborate salt ($HO-(CH_2)_2-C_6H_4-N_2^+$) using chronoamperometry in acetonitrile with 0.1 M $^+N_2Bu_4BF_4$ salt at −0.7 V/SCE for 30 s. Hydroxyl (−OH)-terminated aryl moieties covalently anchored to the surface are formed. (ii) Esterification of the −OH groups with 2-bromopropionyl bromide (0.1 M in dichloromethane, in the presence of triethylamine at 0.12M) is achieved to produce bromo-terminated aryl-grafted groups, which are essential entities to initiate NIPAM polymerization. The surface coverage has been estimated to 9 molecules/nm^2 by XPS spectroscopy, which appears to be high enough to allow the growth of dense polymer layers.[31] This two-step alternative route ensures a linker strongly tethered to the underlying gold substrate by one end, as previously reported.[32−35] (iii) PNIPAM brushes are grown from the initiator-covered substrate using standard aqueous surface-initiated atom-transfer radical polymerization (SI-ATRP) conditions for 10 min at room temperature. This procedure allows accurate control of the PNIPAM thickness, homogeneity, and grafting density. Recent works from our group revealed that this two-step strategy allows grafting of dense polymer layers in a brush regime at room temperature.[31]

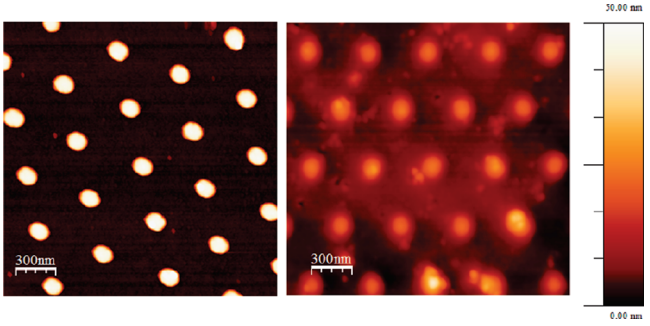

Figure 2. (left) AFM image of the lithographic gold nanoparticle array deposited on the ITO substrate. (right) AFM image of the PNIPAM-coated NP array. The AFM images are recorded in air in tapping mode.

After the polymerization process, the AFM images reveal that the particles are completely covered by the PNIPAM and that the polymer brushes are smooth and homogeneous (Figure 2). Note that the PNIPAM brushes are attached on both the gold NPs and the ITO substrate. In a dry state, the PNIPAM thickness was estimated by AFM scratch measurements on ITO to be ∼25 ± 5 nm. Recent work by L. Bureau et al. has shown that in dry conditions, the thickness of the PNIPAM chains is close to that measured in water for a collapsed regime (above the LCST).[29] Moreover, our recent studies highlighted a swelling ratio α of ∼6 (α representing the ratio between the swollen brush thickness and the collapsed brush thickness). Therefore, it provides a swollen PNIPAM brushes thickness at around 150 ± 5 nm below the LCST.

The LSPR resonance of these hybrid systems was probed by using far-field visible−NIR extinction microspectroscopy in the range of 500−900 nm. The spectrometer (LOT ORIEL model MS 260i) was coupled to an optical microscope (OLYMPUS BX 51) equipped with a 50× objective (numerical aperture N.A.# 0.75) for experiments in air and a 100× objective (N.A.#1) for experiments in water. The investigated area was a circle of approximately 80 μm diameter when using the 50× objective and 40 μm when using the 100× objective, which was smaller

dx.doi.org/10.1021/jz200272r |*J. Phys. Chem. Lett.* 2011, 2, 926–931

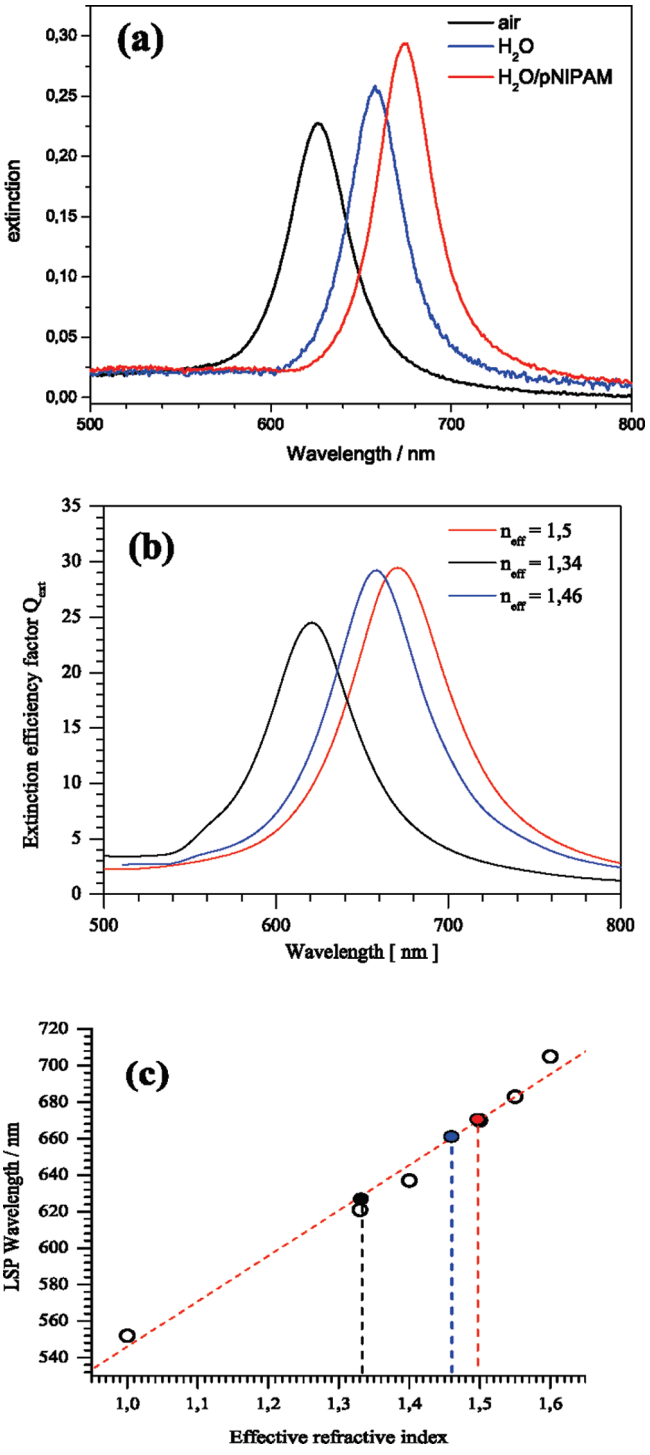

Figure 3. (a) Extinction spectra of the gold NP array recorded in air at room temperature (black), in water (blue), and in water with PNIPAM below the LCST (red). (b) Calculated extinction factor efficiencies of the gold NP array deduced from the DDA method (see text). (c) LSPR wavelength versus the effective RI deduced from DDA calculations.

than the particle array (100 × 100 μm). Figure 3a displays the extinction spectra of an uncoated gold NP array in air (RI n_{air} = 1, back curve), in water (RI n_{water} = 1.33, blue curve), and after polymerization in water below the LCST (RI n_{PNIPAM} > 1.33, red curve). As expected, a red shift of the LSPR wavelength is observed from 620 nm in air to 670 nm for the PNIPAM-coated NP array in water due to the increase of the surrounding medium RI. We can note that the LSPR bandwidth is not affected by the presence of the polymer chains, which indicates that the LSPR excitation is not damped, despite the polymer grafting.

The DDA method was employed to model the LSPR wavelength shifts as a function of the surrounding medium RI. This method is one particular discretization method for solving Maxwell's equations in the presence of a particle in which the continuum particle is replaced by an array of polarizable *N*-point dipoles located on cubic lattice sites.[36,37] Computations were performed using the DDSCAT 7.0 software, which calculates efficiency factors, $Q_{ext} = C_{ext}/\pi a_{eff}^2$, for regular arrays of particles by using periodic conditions (C_{ext} is the extinction cross section and a the effective radius of the particle). Because, in the present case, the particle array is hexagonal, we chose a unit cell containing two particles to account for the array structure.[36−38] We will not detail further its description because this method is frequently described in the literature.

We first aimed at comparing the experimental spectra with the calculated extinction efficiency factors Q_{ext} displayed in Figure 3. Using periodic limit condition in these calculations, the interactions between NPs are taken into account, enabling us to make reliable comparisons between the experimental and calculated spectra. A good match of the LSPR wavelength and band shape between experimental spectra and the extinction efficiency factors Q_{ext} is obtained for n_{eff} equal to 1.34 in air, 1.46 in water, and 1.50 in PNIPAM medium (Figure 3a and b). Finally, a linear dependence between the LSPR wavelength and n_{eff} is observed, as already pointed out in the recent literature (Figure 3c).[39]

The estimation of the PNIPAM RI was deduced from the equation[40,41]

$$n_{eff} = \alpha \times n_{medium} + (1 - \alpha) n_{ITO} \quad (1)$$

where α represents a weighting factor ($0 < \alpha < 1$), n_{medium} is the surrounding medium RI, and n_{ITO} is the RI of the ITO substrate (equal to ~2). The value of α was deduced as follows: by varying n_{eff} in the DDA calculation, one can match the LSPR wavelength between the experimental extinction spectra and calculated ones. For instance, good agreement is obtained for the extinction spectrum in water (n_{water} = 1.33), with a LSPR maximum at 658 nm, when considering an effective RI value of n_{eff} = 1.46 in the calculation. Thus, from the RI values n_{water} and n_{eff}, it is possible to deduce the value of the weighting factor using eq 1; we found α to be equal to 0.8. This means that the LSPR maximum position is mostly affected by the RI of water, which is realistic because the NPs are deposited and not embedded in the ITO substrate. Therefore, from eq 1, a RI of 1.37 was deduced when considering the PNIPAM layer in water below the LCST.[42]

When the PNIPAM-coated NP array is immersed in water and heated from 20 to 50 °C (above the LCST), the LSPR wavelength is red-shifted from 670 to 680 nm, as shown in Figure 4a. The 10 nm red shift is attributed to the collapse of the brushes, leading to an increase of both the polymer density close to the NPs and the surrounding medium RI. From the DDA calculations described above, we found a RI of the PNIPAM at the collapsed state of 1.43 (T > LCST). The 10 nm red shift thus results in a variation Δn of the local RI of 0.06.

Figure 4b displays the dependence of the LSPR wavelength when the temperature varies between 18 and 52 °C. The swelling−deswelling behavior of PNIPAM brushes with temperature variations is clearly observed with a LCST at 32 °C, as

dx.doi.org/10.1021/jz200272r |*J. Phys. Chem. Lett.* 2011, 2, 926–931

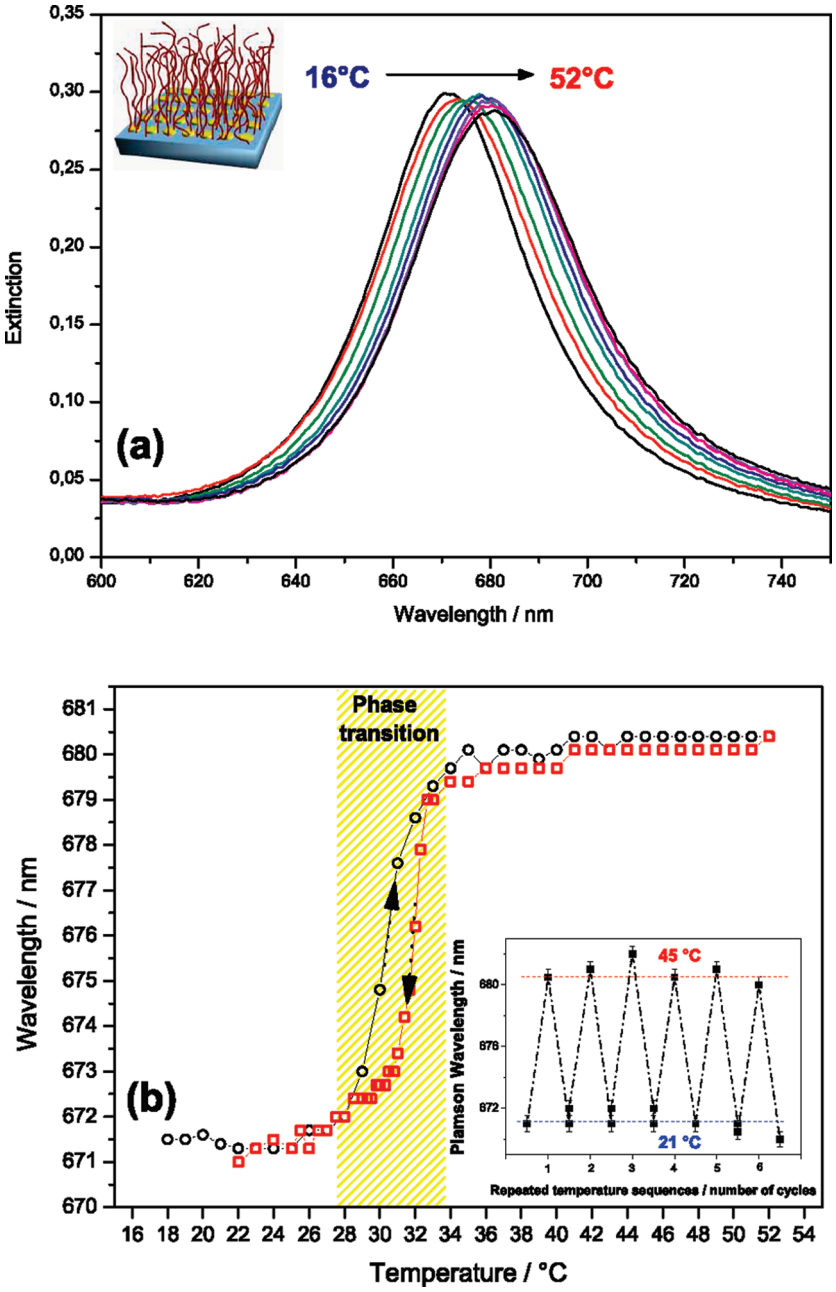

Figure 4. (a) Set of eight extinction spectra of the PNIPAM-coated NP arrays going from 16 to 52 °C. The LSP band maximum at the smallest wavelength has been recorded at 16 °C, while the LSP band maximum at the highest wavelength has been recorded at 52 °C. (b) Extinction wavelength at the maximum versus the temperature from 18 to 52 °C. (Inset) Variation of the LSP wavelength of the PNIPAM-coated NP array in water as a function of the external temperature for repeated temperature cycles (from 21 to 45 °C).

expected for such a thermosensitive polymer.[23] More importantly, the LCST phase transition region is sharp (around 6 °C) and steep, as compared to gold hybrid colloidal systems (around 15 °C).[43] Such an abrupt transition is an added value for the elaboration of improved thermoswitchable devices. When decreasing the temperature from 52 to 18 °C, the LSPR wavelength is blue-shifted to its initial value, indicating fully reversible behavior of the PNIPAM. The hysteresis observed during one heating−cooling cycle is due to the formation of inter- and intrachain hydrogen bonding between >C═O and H−N< groups above the LCST. This process acts as "cross-linking" points, modifying the swelling cycle.[44,45] Note that the stability of our system has been checked through more than 20 cycles in temperature, indicating that the links between all of the components are strong, therefore making our plasmonic device very stable (inset in Figure 4b).

In summary, thermosensitive plasmonic lithographic gold/polymer structures combining calibrated arrays of gold NPs and stimuli-responsive polymer brushes were successfully designed. Such arrays display a very narrow LSPR band, leading to a fine-tuning of their optical response through the change of temperature. The RI of the PNIPAM chains in water below and above the LCST was determined using the DDA method. The linear dependence between the LSPR wavelength and the effective RI

dx.doi.org/10.1021/jz200272r |J. Phys. Chem. Lett. 2011, 2, 926–931

can be used to precisely follow the sharp variation of the RI of the NP surrounding medium around the phase transition. Our strategy can be applied to attach other stimuli-responsive polymer brushes on the lithographic system providing an efficient nanosensor lab-on-chip. Finally, in the context of surface-enhanced spectroscopies such as fluorescence and Raman scattering, such systems provide an original tool for future experiments in order to dynamically study the dependence of the field enhancement factor with the distance between lithographic NPs and dyes attached to the end of the thermosensitive polymer brushes.

AUTHOR INFORMATION

Corresponding Author

*E-mail:nordin.felidj@univ-paris-diderot.fr.

ACKNOWLEDGMENT

The authors gratefully acknowledge the financial support from Ministère de la Défense, Direction Générale de l'Armement DGA (Project DGA-REI 07 34024 and Ph.D. support 2007–2010).

REFERENCES

(1) Kreibig, U.; Vollmer, M. In *Optical Properties Of Metal Clusters*; Springer: New York, 1995.

(2) Krenn, J. R.; Weeber, J. C.; Dereux, A. In *Nanophotonics with Surface Plasmons (Advances In Nano-Optics and Nano-Photonics*; Shalaev, V. M., Kawata, S., Eds.; Elsevier: New York, 2007.

(3) Moskovits, M. Surface-Enhanced Spectroscopy. *Rev. Mod. Phys.* **1985**, *57*, 783–826.

(4) Felidj, N.; Aubard, J.; Levi, G.; Krenn, J. R.; Hohenau, A.; Schider, G.; Leitner, A.; Aussenegg, F. R. Optimized Surface-Enhanced Raman Scattering on Gold Nanoparticle Arrays. *Appl. Phys. Lett.* **2003**, *82*, 3095.

(5) Le Ru, E.; Etchegoin, P.; Grand, J.; Felidj, N.; Aubard, J.; Lévi, G. Mechanisms of Spectral Profile Modification in Surface-Enhanced Fluorescence. *J. Phys. Chem.C* **2007**, *11*, 16076–16079.

(6) Djaker, N; Hostein, R; Devaux, E; Ebbesen, T.; Rigneault, H; Wenger, J. Surface Enhanced Raman Scattering On A Single Nanometric Aperture. *J. Phys. Chem. C* **2010**, *114*, 16250–16256.

(7) Boca, S.; Astilean, S. Detoxification of Gold Nanorods by Conjugation with Thiolated Poly(ethylene glycol) and their Assessment as SERS-Active Carriers of Raman Tags. *Nanotechnology* **2010**, *21*, 235601.

(8) Wurtz, G.; Evans, P.; Hendren, W.; Atkinson, R.; Dickson, W.; Pollard, R.; Zayats, A. Molecular Plasmonics with Tunable Exciton–Plasmon Coupling Strength in J-Aggregate Hybridized Au Nanorod Assemblies. *Nano Lett.* **2007**, *7*, 1297–1303.

(9) Zheng, Y.; Yang, Y.; Jensen, L.; Fang, L.; Juluri, B.; Flood, A.; Weiss, P.; Stoddart, J.; Huang, T. Active Molecular Plasmonics: Controlling Plasmon Resonances with Molecular Switches. *Nano Lett.* **2009**, *9*, 819–825.

(10) Leroux, Y. R.; Lacroix, J. C.; Chane Ching, K. I.; Fave, C.; Felidj, N.; Levi, G.; Aubard, J.; Krenn, J. R.; Hohenau, A. Conducting Polymer Electrochemical Switching as an Easy Means for Designing Active Plasmonic Devices. *J. Am. Chem. Soc.* **2005**, *127*, 16022.

(11) Leroux, Y.; Lacroix, J. C.; Fave, C.; Stockhausen, V.; Felidj, N.; Grand, J.; Hohenau, A.; Krenn, J. R. Active Plasmonic Devices with Anisotropic Optical Response: A Step Toward Active Polarizer. *Nano Lett.* **2009**, *9*, 2144.

(12) Hsiao, V.; Zheng, Y.; Juluri, B.; Huang, T. Light-Driven Plasmonic Switches Based on Au Nanodisk Arrays and Photoresponsive Liquid Crystals. *Adv. Mater.* **2008**, *20*, 3528–3532.

(13) Berthelot, J.; Bouhelier, A.; Huang, C.; Margueritat, J.; Colas Des Francs, G.; Finot, E.; Weeber, J.-C.; Dereux, A.; Kostcheev, S.; E-Ahrach, H. I.;Tuning of an Optical Dimer Nanoantenna by Electrically Controlling Its Load Impedance. *Nano Lett.* **2009**, *9*, 3914–3921.

(14) Cohen Stuart, M. A.; S. Huck, W. T.; Genzer, J.; Müller, M.; Ober, C.; Stamm, M.; Sukhorukov, G. B.; Szleifer, I.; Tsukruk, M.; Urban, V. V.;Emerging Applications of Stimuli-Responsive Polymer Materials. *Nat. Mater.* **2010**, *9*, 101–113.

(15) Minko, S. Responsive Polymer Brushes. *J. Macromol. Sci., Part C* **2006**, *46*, 397–420.

(16) Stuart, M.; Huck, W.; Genzer, J; Muller, M; Ober, C.; Stamm, M; Sukhorukov, G; Szleifer, I.; Tsukruk, W.; Urban, M;Emerging Applications of Stimuli-Responsive Polymer Materials. *Nat. Mater.* **2010**, *9*, 101–113.

(17) Tokarev, I.; Tokareva, I.; Gopishetty, V.; Katz, E.; Minko, S. Specific Biochemical-to-Optical Signal Transduction by Responsive Thin Hydrogel Films Loaded with Noble Metal Nanoparticles. *Adv. Mater.* **2010**, *22*, 1412–1416.

(18) Pita, M.; Tam, T. K.; Minko, S.; Katz, E. Dual Magnetobiochemical Logic Control of Electrochemical Processes Based on Local Interfacial pH Changes. *ACS Appl. Mater. Interfaces* **2009**, *1*, 1166–1168.

(19) Tokareva, I.; Minko, S.; Fendler, J. H.; Hutter, E. Nanosensors Based on Responsive Polymer Brushes and Gold Nanoparticle Enhanced Transmission Surface Plasmon Resonance Spectroscopy. *J. Am. Chem. Soc.* **2004**, *126*, 15950–15951.

(20) Tokareva, I.; Tokarev, I.; Minko, S.; Hutter, E.; Fendler, J. H. Ultrathin Molecularly Imprinted Polymer Sensors Employing Enhanced Transmission Surface Plasmon Resonance Spectroscopy. *Chem. Commun.* **2006**, 3343–3345.

(21) Tokarev, I.; Tokareva, I.; Minko, S. Gold-Nanoparticles-Enhanced Plasmonics Effects in a Repsonsive Polymer Gel. *Adv. Mater.* **2008**, *20*, 2730–2734.

(22) Kim, S.; Cheng, N.; Jeong, J. R.; Jang, S.; Yang, S.; Huck, W. Localized Surface Plasmon Resonance (LSPR) Sensitivity of Au Nanodot Patterns to Probe Solvatation Effects in Polyelectrolyte Brushes. *Chem. Commun.* **2008**, 3666–3668.

(23) Sanchez-Iglesias, A.; Grzelczak, M.; Rodriguez-Gonzalez, B.; Guardia Giros, P.; Pastoriza-Santos, I.; Perez-Juste, J.; Prato, M.; Liz-Marzan, L. Synthesis of Multifunctional Composite Microgels via In-situ Ni Growth on PNIPAM-Coated Au Nanoparticles. *ACS Nano* **2009**, *3*, 3184–3190.

(24) Karg, M.; Lu, Y.; Carbo-Argibay, E.; Pastoriza-Santos, I.; Perez-Juste, J.; Liz-Marzan, L.; Hellweg, T. Multirepsonsive Hybrid Colloids Based on Gold Nanorods and Poly(NIPAM-co-allylacetic acid) Microgels: Temperature- and pH-Tunable Plasmon Resonance. *Langmuir* **2009**, *25*, 3163–3167.

(25) Karg, M.; Pastoriza-Santos, I.; Perez-Juste, J.; Hellweg, T.; Liz-Marzan, L. Nanorod-Coated PNIPAM Microgels: Thermoresponsive Optical Properties. *Small* **2007**, *3*, 1222–1229.

(26) Lu, Y.; Mei, Y.; Drechsler, M.; Ballauff, M. Thermosensitive Core–Shell Particles as Carriers for Ag Nanoparticles: Modulating the Catalytic Activity by a Phase Transition in Networks. *Angew. Chem., Int. Ed.* **2006**, *45*, 813–816.

(27) Dong, H.; Zhu, M.; Yoon, J.; Gao, H.; Jin, R.; Matyjaszewski, K. One-Pot Synthesis of Robust Core/Shell Gold Nanoparticles. *J. Am. Chem. Soc.* **2008**, *130*, 12852–12853.

(28) Gupta, S.; Agrawal, M.; Uhlmann, P.; Simon, F.; Stamm, M. Poly(*N*-isopropyl acrylamide)–Gold Nanoassemblies on Macroscopic Surfaces: Fabrication, Characterization, and Application. *Chem. Mater.* **2010**, *22*, 504–509 and references therein.

(29) Malham, I. B.; Bureau, L. Density Effects on Collapse, Compression, and Adhesion of Thermoresponsive Polymer Brushes. *Langmuir* **2010**, *26*, 4762–4768.

(30) McCord, M. A.; Tooks, M. J. In *Handbook of Mcrolithography, Micromachining and Microfabrication*; Rai-Choudhury, P., Ed.; SPIE: Bellingham, WA, 1997; Vol. 1, Chapter 2, pp 139–249.

(31) Gehan, H.; Fillaud, L.; Chehimi, M.; Aubard, J.; Hohenau, A.; Felidj, N.; Mangeney, C. Thermo-Induced Electromagnetic Coupling in

Gold/Polymer Hybrid Plasmonic Structures Probed by Surface-Enhanced Raman Scattering. *ACS Nano* **2010**, *4*, 6491–6500.

(32) Love, J.; Estroff, L.; Kriebel, J.; Nuzzo, R.; Whitesides, G. Self-Assembled Monolayers of Thiolates on Metals as a Form of Nanotechnology. *Chem. Rev.* **2005**, *105*, 1103–1170.

(33) Mack, N.; Wackerly, J.; Malyarchuk, V.; Rogers, J.; Moore, J.; Nuzzo, R. Optical Transduction of Chemical Forces. *Nano Lett.* **2007**, *7*, 733–737.

(34) Pinson, J.; Podvorica, F. Attachment of Organic Layers to Conductive or Semiconductive Surfaces by Reduction of Diazonium Salts. *Chem. Soc. Rev.* **2005**, *34*, 429–439.

(35) Liu, G. Z.; Böcking, T.; Gooding, J. J. Diazonium Salts: Stable Monolayers on Gold Electrodes for Sensing Applications. *J. Electroanal. Chem.* **2007**, *600*, 335–344.

(36) Purcell, E. M.; Pennypacker, C. R. Scattering and Absorption of Light by Nonspherical Dielectric Grains. *Astrophys. J.* **1973**, *186*, 705–714.

(37) Draine, B. T. The Discrete-Dipole Approximation and its Application to Interstellar Graphite Grains. *Astrophys. J.* **1988**, *333*, 848–872.

(38) Yang, W.-H.; Schatz, G. C.; Van Duyne, R. P. Discrete Dipole Approximation for Calculating Extinction and Raman Intensities for Small Particles with Arbitrary Ahapes. *J. Chem. Phys.* **1995**, *103*, 869–875.

(39) Sherry, L. J.; Jin, R.; Mirkin, C. A.; Schatz, G. C.; Van Duyne, R. P. Localized Surface Plasmon Resonance Spectroscopy of Single Silver Triangular Nanoprisms. *Nano Lett.* **2006**, *6*, 2060–2065.

(40) Curry, A.; Nusz, G.; Chilkoti, A.; A. Wax, A. Substrate Effect on Refractive Index Dependence of Plasmon Resonance for Individual Silver Nanoparticles Observed Using Darkfield Micro-Spectroscopy. *Opt. Lett.* **2005**, *13*, 2668–2677.

(41) Gotchy, W.; Vonmetz, K.; Leitner, A.; Aussenegg, F. R. Thin Films by Regular Patterns of Metal Nanoparticles: Tailoring the Optical Properties by Nanodesign. *Appl. Phys. B: Lasers Opt.* **1996**, *63*, 381.

(42) Mitsuishi, M.; Koishikawa, Y; Tanaka, H.; Sato, E.; Mikayama, T.; Matsui, J.; Miyashita, Y. Nanoscale Actuation of Thermoreversible Polymer Brushes Coupled with Localized Surface Plasmon Resonance of Gold Nanoparticles. *Langmuir* **2007**, *23*, 7472–7474.

(43) Contreras-Caceres, R.; Sanchez-Iglesias, A.; Karg, M.; Pastoriza-Santos, I.; Perez-Juste, J.; Pacifico, J.; Hellweg, T.; Fernandez-Barbero, A.; Liz-Marzan, L. M. Encapsulation and Growth of Gold Nanoparticles in Thermoresponsive Microgels. *Adv. Mater.* **2008**, *20*, 1666–1670.

(44) Cheng, H.; Shen, L.; Wu, C. LLS and FTIR Studies on the Hysteresis in Association and Dissociation of Poly(*N*-isopropylacrylamide) Chains in Water. *Macromolecules* **2006**, *39*, 2325–2329.

(45) Lu, Y.; Zhou, K.; Ding, Y.; Zhang, G.; Wu, C. Origin of Hysteresis Observed in Association and Dissociation of Polymer Chains in Water. *Phys. Chem. Chem. Phys.* **2010**, *12*, 3188–3194.